



ISSN: 0975-833X

RESEARCH ARTICLE

MOLECULAR CONFORMATIONAL STABILITY AND SPECTROSCOPIC ANALYSIS OF N-((3-BROMO-1-(PHENYLSULFONYL)-1H-INDOL-2-YL) METHYL)ACETAMIDE WITH EXPERIMENTAL AND QUANTUM CHEMICAL CALCULATIONS

¹Srinivasaraghavan, R., ²Seshadri, S., ³Gnanasambandan, T. and ⁴Srinivasan, G.

¹Department of Physics, SCSVMV University, Enathur, Kanchipuram 631 561, India

²Department of Physics, L.N. Govt. College, Ponneri 601 204, India

³Department of Physics, Pallavan College of Engineering, Kanchipuram-631502, India

⁴Department of Physics, Govt. College for Men, Nandanam, Chennai, India

ARTICLE INFO

Article History:

Received 12th April, 2015

Received in revised form

26th May, 2015

Accepted 30th June, 2015

Published online 31st July, 2015

Key words:

N3BP2MA, PED, NBO, NLMO, MEP

ABSTRACT

The complete vibration analysis of the fundamental modes of N-((3-Bromo-1-(phenylsulfonyl) -1H-indol-2-yl) methyl) acetamide (N3BP2MA) was carried out using the experimental FTIR and FT-Raman data and quantum chemical studies. The observed vibrational data were compared with the wavenumbers derived theoretically from the optimized geometry of the compound from the DFT-B3LYP gradient calculations employing 6-31G (2d, 3p) and 6-311++G (2d, 3p) basis sets. Thermodynamic properties like entropy, heat capacity and enthalpy were calculated for the molecule and the HOMO-LUMO energy gap was calculated. The intramolecular contacts had been interpreted using natural bond orbital (NBO) and natural localized molecular orbital (NLMO) analysis. Important non-linear properties such as electric dipole moment and first hyperpolarizability of N3BP2MA were computed using B3LYP quantum chemical calculations. Finally, the Mulliken population analysis on atomic charges of the title compound were calculated.

Copyright © 2015 Srinivasaraghavan et al. This is an open access article distributed under the Creative Commons Attribution License, which permits unrestricted use, distribution, and reproduction in any medium, provided the original work is properly cited.

Citation: Srinivasaraghavan, R., Seshadri, S., Gnanasambandan, T. and Srinivasan, G. 2015. "Molecular conformational stability and spectroscopic analysis of n-((3-bromo-1-(phenylsulfonyl)-1h-indol-2-yl)methyl)acetamide with experimental and quantum chemical calculations", *International Journal of Current Research*, 7, (7), 18383-18400.

INTRODUCTION

N-((3-Bromo-1-(phenylsulfonyl)-1H-indol-2-yl) methyl) acetamide is otherwise called (N3BP2MA). Indole derivatives exhibit antibacterial, antifungal (Singh *et al.*, 2000) and antitumor activities (Andreani *et al.*, 2001). These derivatives also exhibit antimicrobial, antibiotic, analgesic, anticancer and anti-HIV (Pomarnacka and Kozlarska-Kedra, 2003; Srivastava, and Pandeya, 2011) activities. The Compound was synthesized by A.K. Mohanakrishnan *et al.* (2013) and no further studies have been carried out for the title compound yet. Especially, Studies related to vibrational spectroscopic investigation and assignments using ab initio and dft techniques for the title compound are not reported and analyzed in the literature. Hence, in this study, we set out experimental and theoretical investigation of the vibrational and electronic transitions of N3BP2MA. In the ground state theoretical geometrical parameters, IR and Raman spectra, HOMO and LUMO energies of title molecule were calculated by using Gaussian 03W program.

Detailed interpretations of the vibrational spectra of the N3BP2MA have been made on the basis of the calculated potential energy distribution (PED). The experimental results (IR and Raman spectra) were supported by the computed results, comparing with experimental characterization data; vibrational wave numbers are in fairly good agreement with the experimental results. The redistribution of electron density (ED) in various bonding, antibonding orbitals and E (2) energies have been calculated by natural bond orbital (NBO) / Natural Localized Molecular Orbital (NLMO) analysis to give clear evidence of stabilization originating from the hyper conjugation of various intra-molecular interactions. By analyzing the density of states, the molecular orbital compositions and their contributions to the chemical bonding were studied. The study of HOMO, LUMO analysis has been used to elucidate information regarding charge transfer within the molecule. Moreover, the Mulliken population analyses of the title compound have been calculated and the results have been reported. The experimental and theoretical results supported each other, and the calculations are valuable for providing a reliable insight into the vibrational spectra and molecular properties.

*Corresponding author: Seshadri

Department of Physics, L.N. Govt. College, Ponneri 601 204, India.

Experimental

The compound *N*-((3-Bromo-1-(phenylsulfonyl)-1*H*-indol-2-yl)methyl)acetamide (N3BP2MA) was a synthesized one and reported in Literature (Umadevi *et al.*, 2013) and used as such without further purification to record FTIR and FT Raman spectra. The FTIR spectrum of the compounds is recorded in the region 4000 – 400 cm⁻¹ in evacuation mode on Bruker IFS 66V spectrophotometer using KBr pellet technique (solid phase) with 4.0 cm⁻¹ resolutions. The FT-Raman spectra of these compounds are also recorded in the same instrument with FRA 106 Raman module equipped with Nd: YAG laser source operating at 1.064 μm line widths with 200 mW power. The spectra are recorded in the range of 3500–100 cm⁻¹ with scanning speed of 30 cm⁻¹ min⁻¹ of spectral width 2 cm⁻¹. The frequencies of all sharp bands are accurate to ±1 cm⁻¹. The spectral measurements were carried out at Sophisticated Analytical Instrumentation Facility, IIT, Chennai, India.

Computational details

A complete information regarding the structural characteristics and the fundamental vibrational modes of *N*-((3-Bromo-1-(phenylsulfonyl)-1*H*-indol-2-yl)methyl)acetamide (N3BP2MA), has been carried out using the B3LYP correlation functional calculations. The calculations of geometrical parameters in the ground state were performed using the Gaussian 09 (Frisch *et al.*, 2004) program. DFT calculations were carried out with Becke's three-parameter hybrid model (Becke, 1993) using the Lee–Yang–Parr correlation (Lee *et al.*, 1988) functional (B3LYP) method. The geometry optimization was carried out using the initial geometry generated from standard geometrical parameters of the B3LYP method with 6-31G (2d, 3p) and 6-311++G (2d, 3p) basis sets. The optimized geometry was determined by minimizing the energy with respect to all geometrical parameters without imposing molecular symmetry constraints. Harmonic vibrational wavenumbers were calculated using analytic second derivatives to confirm the convergence to minima in the potential surface. At the optimized structure of the examined species, no imaginary wavenumber modes were obtained, proving that a true minimum on the potential surface was found. The calculated frequencies are scaled according to the work of Rauhut and Pulay (Pulay *et al.*, 1983; Rauhut and Pulay, 1995), a scaling factor of 0.9613 was used for both basis sets. According to Scaled Quantum Mechanics (SQM) procedure using selectively scaling in the natural internal coordinate representation (Fogarasi *et al.*, 1985; Fogarasi *et al.*, 1992), the transformation of force field; subsequent normal coordinates analysis and calculation of the Potential Energy Distribution (PED) were done on a PC with the MOLVIB program (version V7.0-G77) written by Sundius (Sundius, 1990; Sundius, 2002; MOLVIB, 2002). By the use of the GAUSSVIEW molecular visualization program (Frisch *et al.*, 2000) along with available related molecules; the vibrational frequency assignments were made by their PED with a high degree of confidence. The PED elements provide a measure of each internal coordinate's contribution to the normal coordinates.

Prediction of Raman intensities

The Raman activities (S_i), calculated by the Gaussian 03 programs, were converted to relative Raman intensities (I_i) using the following relationship

$$I_i = \frac{f(v_o - v_i)^4 S_i}{v_i(1 - \exp(-hc v_i/kT))}$$

where v_o is the exciting frequency (in cm⁻¹ units); v_i is the vibrational wave number of the i^{th} normal mode; h , c , k are the universal constants and f is the suitably chosen common scaling factor for all the peak intensities.

RESULTS AND DISCUSSION

Molecular geometries

In order to find the most optimized geometry, the energies were carried out for N3BP2MA, using B3LYP/6-311G(2d,3f) method and basis set for various possible conformers. There are Twelve conformers for *N*-((3-Bromo-1-(phenylsulfonyl)-1*H*-indol-2-yl)methyl)acetamide (N3BP2MA). The computationally predicted various possible conformers obtained for the compound N3BP2MA is shown in Fig. 1. The total energies obtained for these conformers were listed in Table 1.

Table 1. Total energies of different conformations of N3BP2MA calculated at the B3LYP/6-311++G(2d,3p) level of theory

S. No	Conformers	Energy (kJ/Mol)
1	C ₁	327.7877
2	C ₂	344.4413
3	C ₃	930.7399
4	C ₄	393.3612
5	C ₅	449.6941
6	C ₆	364.1442
7	C ₇	416.9442
8	C ₈	327.5515
9	C ₉	1743.7506
10	C ₁₀	366.6712
11	C ₁₁	398.4375
12	C ₁₂	514.3921

It is clear in Table 1, the structure optimizations have shown that the conformer C₁ have produced the global minimum energy of 327.7877KJ/Cal. Therefore, C₁ form is the most stable conformer than the other conformers. The optimized molecular structure with the numbering of atoms of the N3BP2MA is shown in Fig. 2. The most optimized structure parameters of N3BP2MA calculated by DFT-B3LYP levels with the 6-31G(2d,3p) and 6-311++G(2d,3p) basis set are listed in the Table 2 in accordance with the atom numbering scheme given in Fig. 2. The optimized molecular structure of N3BP2MA belongs to C₁ point group symmetry. Table 2 compares the calculated bond lengths and angles for N3BP2MA with those experimentally available from literature value (Ramathilagam *et al.*, 2014).

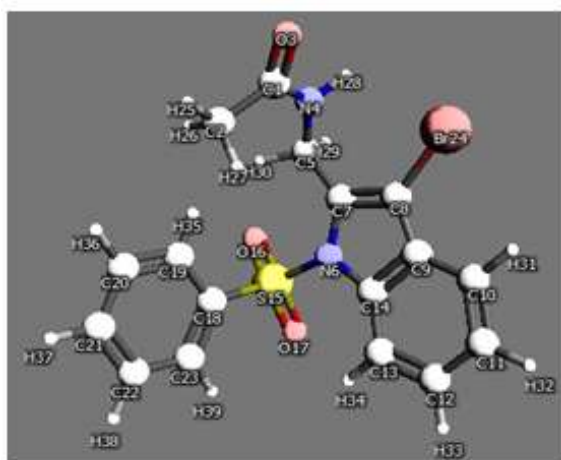
From the theoretical values, we can find that most of the optimized bond angles slightly differ from the experimental values, due to the theoretical calculations belong to isolated molecules in the gaseous phase and the experimental results belong to molecules in the solid state. The theoretical values for the N3BP2MA molecule were compared with the experimental values by means of the root mean square deviation values.

Table 2. Molecular parameters of N3BP2MA

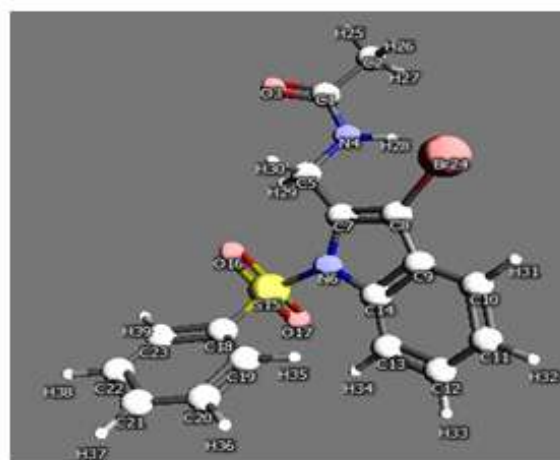
Molecular parameter (Å)	Expt.	6-31g(2d,3p)	6-311++g(2d,3p)
C ₁ -C ₂	1.387	1.410	1.401
C ₁ -O ₃	1.216	1.229	1.218
C ₁ -N ₄	1.420	1.393	1.415
C ₂ -H ₂₅	0.930	1.093	0.987
C ₂ -H ₂₆	0.930	1.093	0.987
C ₂ -H ₂₇	0.930	1.093	0.987
N ₄ -C ₅	1.396	1.428	1.412
N ₄ -H ₂₈	0.980	1.009	0.994
C ₅ -C ₇	1.389	1.413	1.408
C ₅ -H ₂₉	0.930	1.086	0.988
C ₅ -H ₃₀	0.930	1.097	0.988
N ₆ -C ₇	1.396	1.419	1.412
N ₆ -C ₁₄	1.396	1.413	1.412
C ₇ -C ₈	1.388	1.367	1.393
C ₈ -C ₉	1.450	1.438	1.452
C ₈ -Br ₂₄	1.843	1.893	1.839
C ₉ -C ₁₀	1.392	1.401	1.393
C ₉ -C ₁₄	1.392	1.415	1.397
C ₁₀ -C ₁₁	1.388	1.387	1.390
C ₁₀ -H ₃₁	0.930	1.085	0.992
C ₁₁ -C ₁₂	1.392	1.407	1.402
C ₁₁ -H ₃₂	0.930	1.086	0.992
C ₁₂ -C ₁₃	1.392	1.391	1.390
C ₁₂ -H ₃₃	0.980	1.086	0.992
C ₁₃ -C ₁₄	1.384	1.401	1.402
C ₁₃ -H ₃₄	0.980	1.081	0.992
N ₆ -S ₁₅	1.669	1.741	1.753
S ₁₅ -O ₁₆	1.422	1.429	1.426
S ₁₅ -O ₁₇	1.422	1.428	1.425
S ₁₅ -C ₁₈	1.743	1.790	1.746
C ₁₈ -C ₁₉	1.392	1.397	1.395
C ₁₈ -C ₂₃	1.392	1.397	1.392
C ₁₉ -C ₂₀	1.388	1.394	1.390
C ₁₉ -H ₃₅	0.980	1.083	1.105
C ₂₀ -C ₂₁	1.388	1.397	1.397
C ₂₀ -H ₃₆	0.980	1.085	0.992
C ₂₁ -C ₂₂	1.388	1.396	1.394
C ₂₁ -H ₃₇	0.960	1.086	0.992
C ₂₂ -C ₂₃	1.386	1.395	1.394
C ₂₂ -H ₃₈	0.960	1.085	0.992
C ₂₃ -H ₃₉	0.960	1.086	0.992
Bond Angle (°)			
C ₂ -C ₁ -O ₃	121.800	121.300	121.500
C ₂ -C ₁ -N ₄	110.600	113.300	113.200
C ₁ -C ₂ -H ₂₅	109.500	111.900	110.300
C ₁ -C ₂ -H ₂₆	109.500	108.600	110.600
C ₁ -C ₂ -H ₂₇	109.500	108.700	108.700
O ₃ -C ₁ -N ₄	121.100	121.400	121.300
C ₁ -N ₄ -C ₅	122.020	123.300	122.700
C ₁ -N ₄ -H ₂₈	118.080	119.100	118.300
H ₂₅ -C ₂ -H ₂₆	109.500	109.000	109.100
H ₂₅ -C ₂ -H ₂₇	109.500	109.100	109.000
H ₂₆ -C ₂ -H ₂₇	109.500	109.700	109.100
C ₅ -N ₄ -H ₂₈	118.080	117.500	117.300
N ₄ -C ₅ -C ₇	117.000	115.800	116.100
N ₄ -C ₅ -H ₂₉	107.400	107.400	107.400
N ₄ -C ₅ -H ₃₀	107.400	107.900	107.300
C ₇ -C ₅ -H ₂₉	109.500	110.000	109.400
C ₇ -C ₅ -H ₃₀	109.500	110.000	109.300
C ₅ -C ₇ -N ₆	126.500	126.900	126.900
C ₅ -C ₇ -C ₈	126.500	126.300	126.500
H ₂₉ -C ₅ -H ₃₀	109.500	109.500	109.700
C ₇ -N ₆ -C ₁₄	107.600	107.900	107.400
N ₆ -C ₇ -C ₈	110.600	110.800	110.500
N ₆ -C ₁₄ -C ₉	110.600	110.500	110.400
N ₆ -C ₁₄ -C ₁₃	129.700	130.700	130.200
C ₇ -C ₈ -C ₉	112.300	110.700	111.600
C ₇ -C ₈ -Br ₂₄	113.800	115.400	112.800
C ₉ -C ₈ -Br ₂₄	112.900	112.900	112.900
C ₈ -C ₉ -C ₁₀	123.300	123.200	123.500
C ₈ -C ₉ -C ₁₄	115.900	116.100	116.100
C ₁₀ -C ₉ -C ₁₄	119.400	120.700	120.400
C ₉ -C ₁₀ -C ₁₁	117.100	118.500	118.600
C ₉ -C ₁₀ -H ₃₁	119.400	119.800	119.400

Continue.....

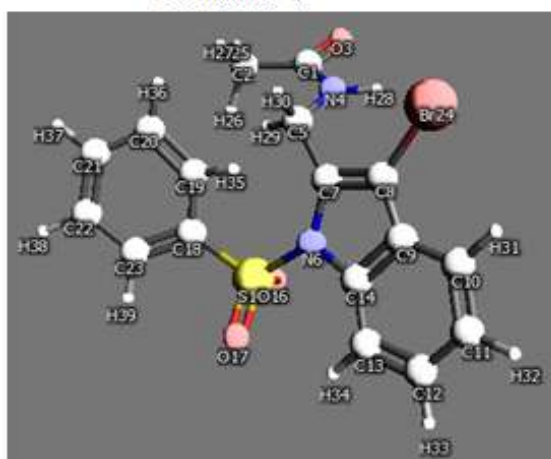
C9-C14-C13	119.100	119.800	119.400
C11-C10-H31	120.500	121.700	121.000
C10-C11-C12	120.500	120.500	121.000
C10-C11-H32	119.400	119.900	119.700
C12-C11-H32	119.400	119.600	119.300
C11-C12-C13	121.900	121.900	121.800
C11-C12-H33	119.400	119.400	119.200
C13-C12-H33	119.000	118.700	119.000
C12-C13-C14	119.000	117.700	117.900
C12-C13-H34	122.000	121.800	121.700
C14-C13-H34	122.000	121.500	121.400
C7-N6-S15	122.020	122.363	122.135
C14-N6-S15	127.030	127.758	127.282
O16-S15-O17	120.110	120.300	120.100
O16-S15-C18	108.500	108.600	108.300
O17-S15-C18	108.500	108.600	108.500
S15-C18-C19	118.700	118.700	118.600
S15-C18-C23	120.300	119.800	120.300
C19-C18-C23	120.700	121.200	120.400
C18-C19-C20	120.400	119.900	120.000
C18-C19-H35	119.800	120.200	119.900
C18-C23-C22	118.300	118.300	118.500
C18-C23-H39	120.700	121.600	120.900
C20-C19-H35	120.700	121.100	120.900
C19-C20-C21	120.400	120.100	120.600
C19-C20-H36	119.600	119.600	120.000
C21-C20-H36	119.600	120.300	120.100
C20-C21-C22	120.400	120.400	120.400
C20-C21-H37	119.600	119.800	119.600
C22-C21-H37	119.600	119.900	119.700
C21-C22-C23	120.700	120.500	120.500
C21-C22-H38	120.000	120.500	120.500
C23-C22-H38	120.000	119.100	119.500
C22-C23-H39	120.000	120.200	119.800



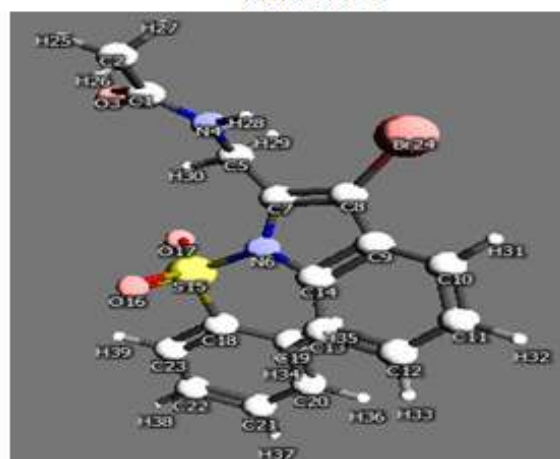
Conformer-1



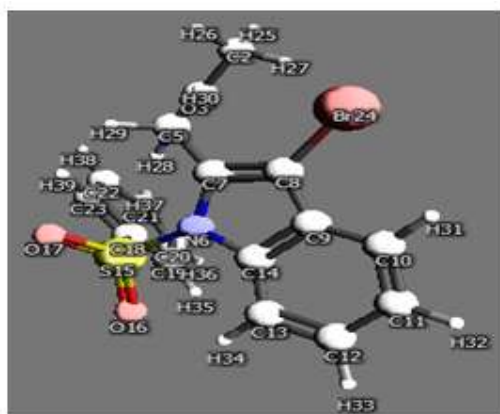
Conformer-2



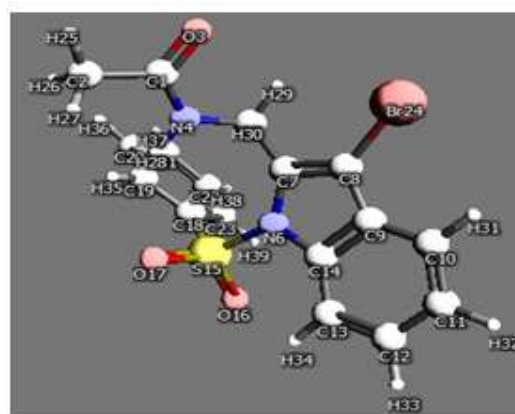
Conformer-3



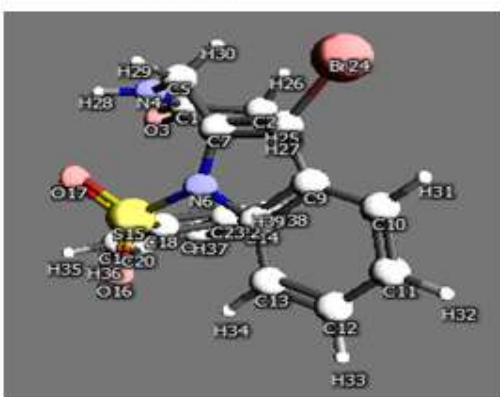
Conformer-4



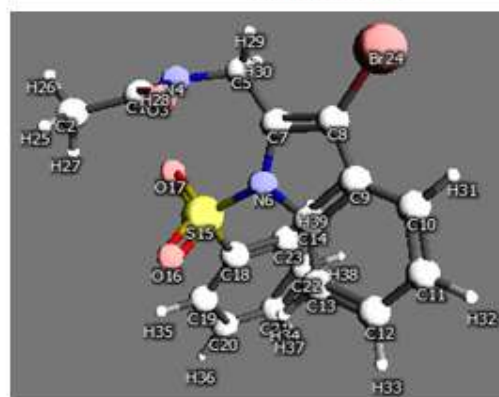
Conformer-5



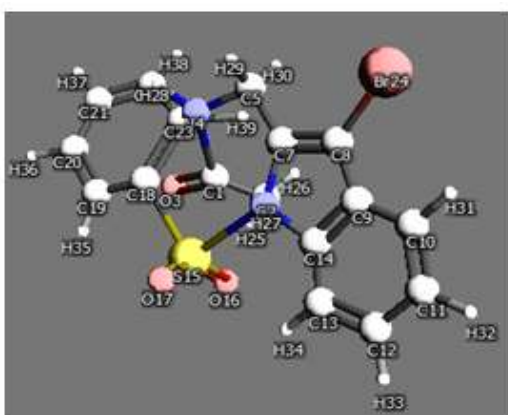
Conformer - 6



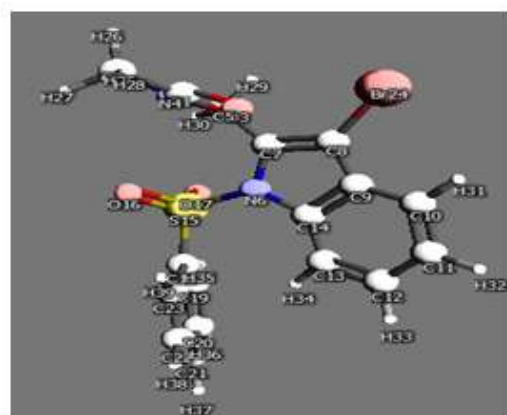
Conformer-7



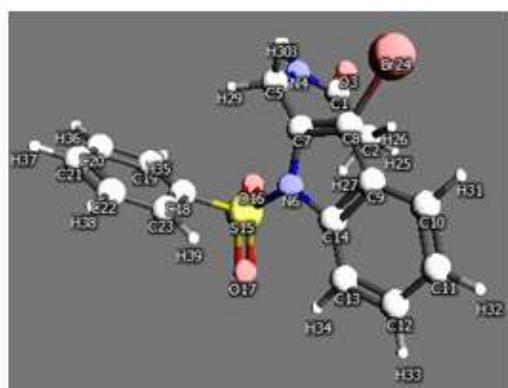
Conformer - 8



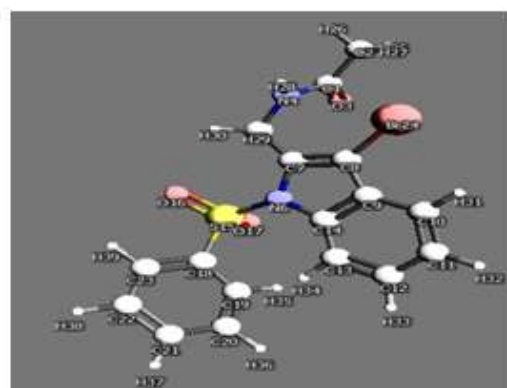
Conformer-9



Conformer - 10



Conformer - 11



Conformer - 12

Fig. 1. Molecular Conformers of N-((3-Bromo-1-(phenylsulfonyl)-1H-indol-2-yl)methyl)acetamide

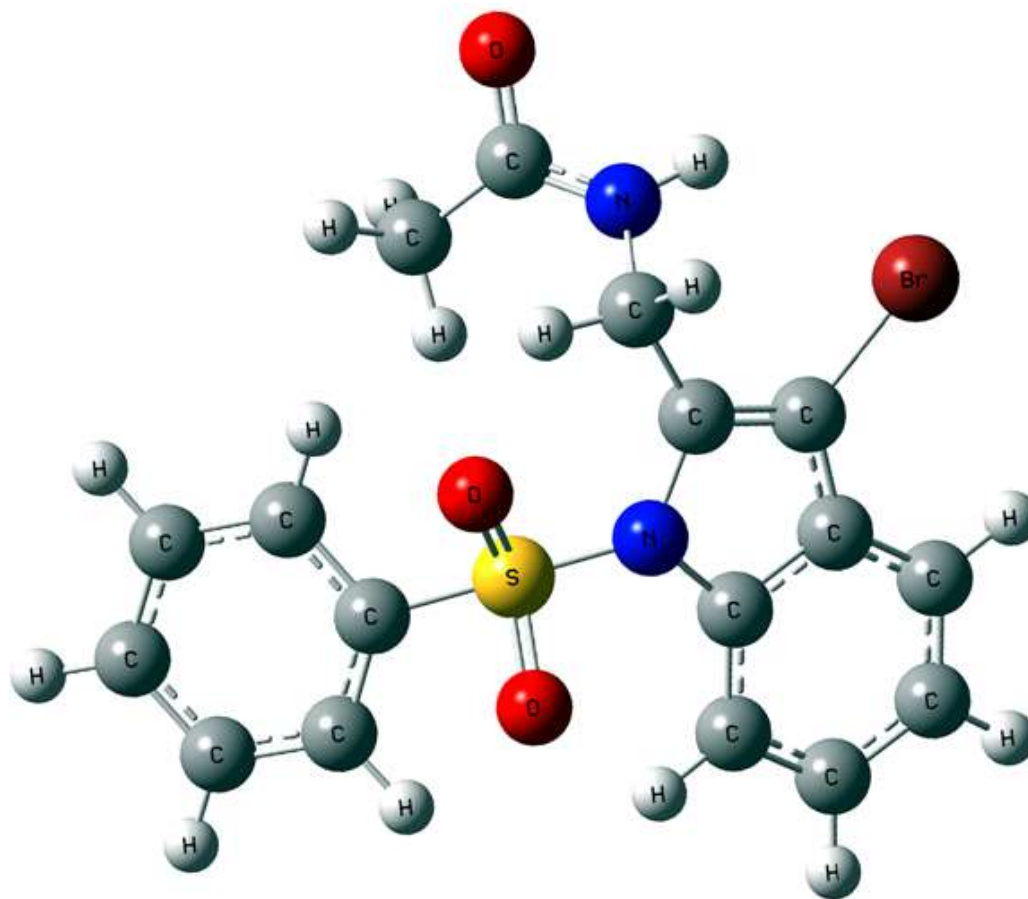


Fig. 2. Optimised Structure of N-((3-Bromo-1-(phenylsulfonyl)-1*H*-indol-2-yl)methyl)acetamide

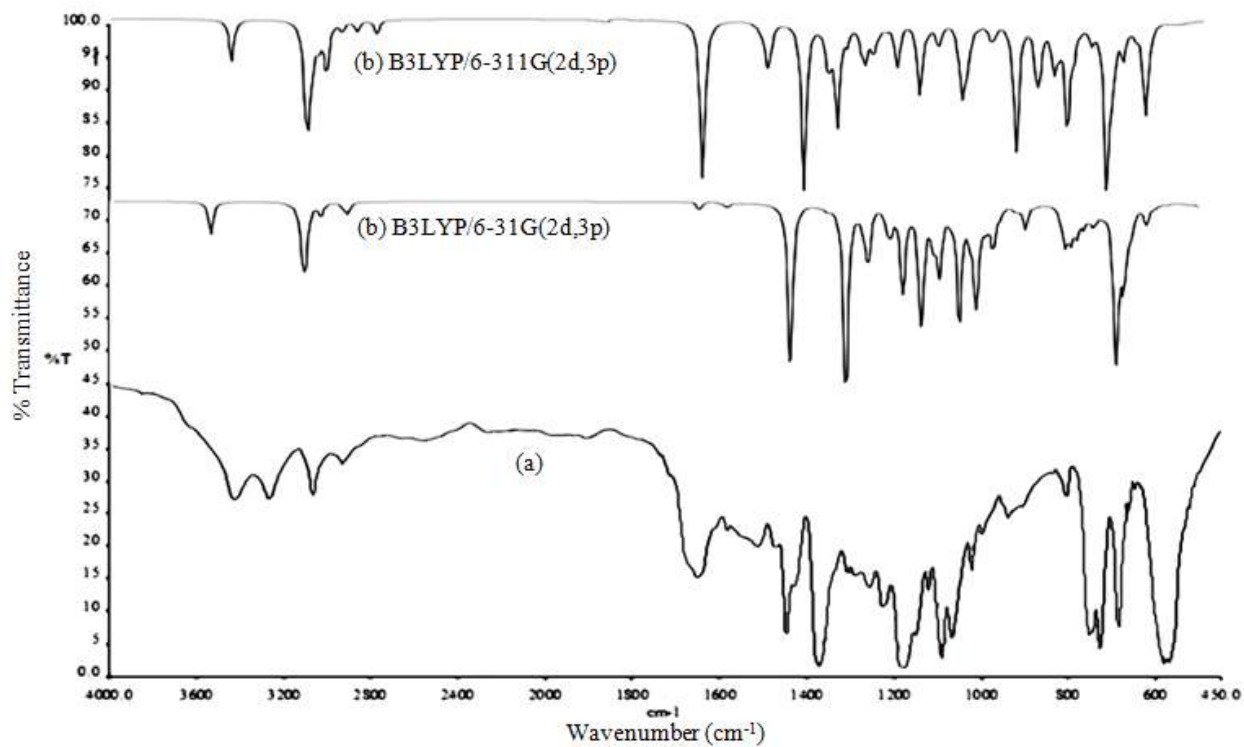


Fig. 3. Comparative (a) Experimental and (b) Theoretical IR spectra of N3BP2MA

Comparing the B3LYP/6-31G(2d,3p) and B3LYP/6-311++G(2d,3p) methods, most of the bond lengths and bond angles are the same in both the methods. The inclusion of diffusion and polarization functions is important to have a better agreement with experimental geometry.

Vibrational assignments

The molecular structure of N3BP2MA belongs to C_1 point group symmetry. For C_1 symmetry there would not be any relevant distribution. The molecule N3BP2MA consists of 39 atoms and expected to have 111 normal modes of vibrations of the same A species under C_1 symmetry. These modes are found to be IR and Raman active, suggesting that the molecule possesses a non-Centro symmetric structure, which recommends the title compound for nonlinear optical applications.

The harmonic vibration modes calculated for N3BP2MA at B3LYP level using the 6-31G (2d, 3p) and 6-311++G (2d, 3p) basis set along with Potential energy distribution has been summarized in Tables 3. The observed FTIR and FT Raman bands for various modes of vibrations of N3BP2MA are assigned and are presented in the Table 3 along with the DFT data. The force fields, thus determined were used to calculate the vibrational potential energy distribution (PED) using the latest version of the MOLVIB program (Sundius, 1990; Sundius, 2002; MOLVIB, 2002). The experimental FT-IR and FT-Raman spectra with corresponding theoretically simulated IR and Raman spectra of N3BP2MA as shown in the Figs. 3 and 4 respectively, where the calculated infrared intensities and Raman intensities are plotted against the vibrational frequencies.

Table 3. Vibrational assignments of N3BP2MA using B3LYP/ 6-31 G(2d,3p) and B3LYP/6-311++G(2d,3p)

vIR cm^{-1}	v Raman cm^{-1}	B3LYP/6-31 G(2d,3p)			B3LYP/6-311++G(2d,3p)			Assignments PED %
		v cm^{-1}	IR intensity	Raman activity	v cm^{-1}	IR intensity	Raman activity	
		10	0.4216	4.7121	12	1.0418	0.2061	τ ring (21)
		19	1.5654	3.8245	20	0.4673	0.4720	β ring (16) + τ CN (61)
		22	0.6552	2.5223	24	2.6101	2.3516	γ SO ₂ (wag) (28)
		43	1.7654	2.7164	42	0.2449	3.2278	β ring (23)
		53	0.3476	5.1528	56	3.8350	1.0723	γ CH ₃ (wag) (25)
		60	0.6391	5.0516	60	0.1801	1.7163	γ SO ₂ (wag) (28)
		85	0.2045	1.7586	85	4.2131	0.8905	γ CC(76)
	107	109	13.3041	1.8342	109	5.7514	0.9341	α CO (38) + β CCN (20)
	120	120	1.5159	2.3386	121	0.2400	0.2073	τ SO ₂ (54)
		131	0.6996	2.2898	132	0.7213	0.9104	α C N (32) + γ CH (17)
	138	139	0.6875	2.5137	139	0.3476	0.9478	τ CH ₃ (46)
	178	177	0.3652	1.3795	176	0.3695	1.1097	β C N (33) + γ CH (9)
	185	185	2.0960	0.6594	184	2.8763	3.3960	τ CH ₃ (51)
	202	203	3.9129	3.0742	202	1.0565	1.6501	τ ring 1 (51)
	212	214	7.5609	2.5085	218	3.6912	0.6818	β NCC(13)
	237	239	2.5027	1.9625	241	2.3465	3.7695	τ CH ₂ (49)
		257	1.9125	3.5759	257	2.5636	0.7539	β CCC(37)
	275	273	3.3964	1.8177	275	1.3342	2.2337	ν CC(24)+ β ring(23)
	308	308	1.8131	4.4542	308	5.5005	6.0495	γ ring 1 (47)
	324	326	1.3972	6.5634	327	5.9013	2.0623	τ ring (12)+ β CCC (15)
		344	0.9570	1.4952	345	4.1203	5.5013	γ CN (16)+ β ring (11)
	365	366	0.3321	2.3684	365	2.8776	11.3111	γ CBr (22)
		372	1.1607	2.3973	371	0.0287	0.8505	τ ring(11)+ β NCH(8)
422	424	424	0.1996	0.0381	423	25.3955	82.4674	γ ring 4 (53) + γ CS (51)
430		430	0.6650	1.9329	430	9.3471	15.5078	δ ring 4 (57)
	438	439	4.6372	0.8870	440	67.1443	0.9770	τ ring (23) + γ CH(12)
445		446	21.2089	2.9780	447	11.6581	61.1047	β Ring (22) + γ CN (11)
471	471	471	9.3126	2.3448	473	22.4293	13.4675	γ CN (69), γ ring 4 (31)
495		497	30.5812	2.9683	497	6.9322	53.1356	δ NS (61), δ ring 4 (34)
520	521	519	44.1479	2.9480	518	71.0353	1.8845	τ NC(13) + β CCO(21)
551	551	552	90.0112	1.8316	551	64.1435	6.0592	β ring (23)
565	562	561	51.1956	1.6999	559	61.2594	7.3414	γ CH(15)+ γ CN(9)
581		580	58.6296	9.2518	576	99.2477	8.2577	ν CS (58)
602	601	601	0.2016	1.1035	600	3.8379	3.6284	γ CO(59)+ τ NC(17)
	624	625	0.7512	5.0927	628	39.4921	6.4323	γ NH (52)
659	659	657	8.3570	3.6517	657	0.5812	2.5605	ν CBr(34)
666	666	668	10.8231	0.5711	665	6.2351	62.4527	γ CC(28)
692		691	22.4580	2.8859	691	55.5692	6.4465	γ CN(26)
710	711	714	11.0872	3.2132	714	96.4832	5.8979	β CCN(24)
742		741	27.1812	0.1758	742	7.4327	57.9460	β NCH(21)
759	760	760	40.5375	6.4225	760	94.1247	9.0256	γ CC(18)
	769	768	47.5406	13.8391	769	11.9223	63.4822	γ CH(21) + ν CS (61)
807	807	809	41.8942	2.2189	809	80.7554	13.6788	β ring(23)
	818	819	17.3823	5.3889	818	2.2567	80.4773	γ CH(86)+ γ CN(8)

Continue.....

821	823	823	10.4006	0.9684	822	58.0721	19.5932	γ CH (43)
892	892	892	1.3312	2.5499	891	99.1386	9.7123	γ CH(79)+vCC(25)
819	819	895	1.1109	8.6146	894	6.9450	49.2934	γ CN(12)
910		915	0.7400	4.3067	914	13.1267	10.4332	γ CC(46)+ τ ring(9)
	965	967	38.4149	6.7900	965	4.0689	19.4882	γ SO(55)
969		970	6.1883	2.0309	969	15.7564	5.6395	γ SO(55)
979	980	983	2.4271	0.6693	982	34.0862	19.9237	vCN(27)+vCC(55)
	988	987	2.1397	0.8753	987	2.2238	7.0738	γ CN(16)
999		999	0.0404	0.1886	998	0.6500	4.9404	γ CH(39)+ γ CC(18)
1006	1006	1005	2.4230	1.9955	1003	1.2913	13.0380	γ CH(33)+ β NCH(15)
1021	1021	1023	10.5889	4.3306	1026	7.4438	4.6136	vCC(47)+vCN(31)
1045		1048	2.8783	22.0082	1049	7.4563	2.9587	γ CO(19)+ β CCH(9)
1057	1057	1060	8.9818	1.2780	1062	46.0706	10.2557	γ CH(38)+ β CCC(24)
	1072	1071	55.2317	3.6640	1070	46.5026	20.2500	vCC(46)+ τ ring(9)
	1079	1080	2.1484	21.1327	1079	27.8678	5.2650	β CCH(46)+vCC(64)
1087	1088	1086	19.2371	23.4257	1084	68.4236	17.9857	β NCH(17)+ β ring(23)
1099	1100	1098	6.6292	0.4929	1100	15.7705	9.5450	δ SO (39)
1157	1156	1159	35.2553	6.5374	1160	23.3439	12.0405	β CCH(18)+ β ring(10)
1170	1168	1168	49.9393	9.0075	1168	34.6322	21.4371	β NCH(21)+ β CCH(16)
	1175	1174	28.3428	4.4171	1174	1.5170	10.9928	vCC(27)+vCN(12)
1195	1195	1198	6.3951	0.7750	1197	2.3398	0.9031	β CCH(64)+vCC(27)
	1204	1200	17.8978	6.4113	1199	4.5820	9.7787	β CCH(37)
1209	1209	1210	67.9502	39.4005	1209	9.5371	7.8455	β CCH(42)+vCC(53)
1229		1228	13.1157	4.5775	1227	35.6376	5.1642	δ CH(53)+ ν _s SO(67)
1237		1236	0.8309	6.5263	1233	70.2370	19.9317	β CCH(18)+ β CCO(11)
1247	1247	1245	0.3211	4.9520	1247	9.1652	7.1968	β CCH(33)+ β CCC(23)
1286	1287	1288	48.2764	2.9280	1287	3.3850	83.3930	β NCH(48)+vCC(41)
1297	1297	1296	49.7561	8.6240	1297	93.5751	15.4960	vCC(87)+ ν _s SO(78)
1305	1301	1301	82.8592	26.8048	1301	15.0321	60.7183	β CCH(80)+vCN(14)
1314	1314	1312	57.8019	5.8915	1311	12.5294	44.3374	vCN(41)+ β CCC(17)
1329	1328	1328	1.8471	1.8567	1329	4.9612	6.8194	vCN(63)
1347	1345	1345	3.7020	0.7354	1346	5.7373	63.8701	vCC(81)+ β CCH(33)
	1354	1354	43.7673	17.1130	1354	9.3890	12.2240	vCN(61)
1356	1356	1358	87.8063	25.2372	1360	7.9856	21.8860	vCC(53)+ β CCH(33)
1368	1367	1370	7.2995	2.7809	1370	33.0696	76.1109	vCC(49)
1398		1396	4.1150	25.0017	1399	22.3910	13.5085	vCC(49)+ β CCC(21)
1401	1401	1400	28.9088	23.2944	1402	39.0947	8.1595	vCN(54)+ β CCC(23)
1410	1410	1413	29.0043	14.5959	1414	42.6485	53.3586	vCN(56)
	1439	1438	56.7877	20.3116	1439	41.2179	4.0575	vCC(79)+ β HCH(13)
1479	1479	1482	6.0874	13.2862	1479	39.6579	53.5582	vCC(49)+ β CCC(21)
1485		1487	23.1564	0.9814	1487	90.3950	17.3050	vCC(51)+ β CCH(33)
1498	1498	1495	7.0817	10.7378	1498	52.3101	80.3220	β HCH(55)+ β CCH(29)
1503	1502	1501	18.7602	13.4344	1503	60.4533	49.3354	β HCH(52)+ β CCH(41)
1520	1520	1520	0.5463	8.1709	1521	7.2742	61.6126	β CCH(33)
	1543	1544	3.2522	1.0837	1547	99.1721	2.8829	β CCH(58)+vCC(47)
1559	1557	1556	99.8014	3.9046	1557	14.2848	0.2133	β CCH(38)+vCC(68)
1579	1580	1578	1.4559	69.0577	1577	1.4106	17.8593	β HCH(59)+ β CCH(37)
1595		1593	4.6307	14.7080	1592	26.1024	1.6864	vCC(47)
1603	1604	1601	2.7272	45.7757	1603	85.5443	6.7973	vCN(89)
1611		1612	0.1685	6.8892	1612	15.6818	0.3681	vCC(83)+ β ring(38)
1630		1631	2.4232	42.9951	1635	3.8518	7.4284	vCC(47)+ β CCH(23)
1647	1646	1648	97.6796	5.6484	1650	99.5094	1.4953	vC=O(61)
2949	2948	2948	17.5213	85.8225	2945	3.6068	99.3736	v CH(94)
3015	3017	3011	6.5953	76.4275	3014	26.4117	8.3335	v CH(97)
3068	3070	3068	5.5389	90.8007	3067	11.5070	40.8032	ν _s CH(96)
3094	3093	3092	15.3744	47.0123	3089	12.4030	47.8987	ν _s CH(97)
3124	3125	3122	2.9410	65.0306	3121	54.4943	12.8866	ν _s CH(99)
3149		3149	3.5618	54.8950	3147	40.9095	2.6700	ν _s CH(98)
3160	3159	3160	11.1324	72.8111	3156	10.6341	7.7189	v CH(98)
3177	3176	3175	11.4237	45.4758	3171	43.3017	1.8323	ν _{as} CH(99)
	3179	3178	23.4241	75.6347	3178	12.2138	43.5650	v CH(99)
3181	3182	3182	7.0773	46.0216	3181	4.9250	38.2696	ν _{as} CH(97)
3187	3187	3186	17.8701	96.5721	3186	2.7135	33.7454	ν _{as} CH(98)
3190		3189	23.9300	98.3412	3188	73.8214	4.0477	ν _{as} CH(99)
3195	3195	3196	1.8096	58.1264	3194	54.5990	6.0723	ν _{as} CH(98)
	3199	3198	1.7544	71.7765	3197	62.0329	7.6999	ν _{as} CH(99)
3460	3459	3457	50.5523	47.2253	3455	97.2356	1.9728	v NH(98)

In the spectra, the theoretically simulated spectra are more regular than the experimental ones because many vibrations presenting in condensed phase lead to strong perturbation of infrared and Raman intensities of many other modes. The RMS error of the observed and calculated frequencies (unscaled) of N3BP2MA is quite obvious since the frequencies are calculated on the basis of quantum mechanical force fields usually differ appreciably from observed frequencies. This is partly due to the neglect of anharmonicity and partly due to the approximate nature of the quantum mechanical methods. In order to reproduce the calculated frequencies, the scale factors were refined and optimized via a least squares refinement algorithm.

N-H vibrations

Primary aliphatic amines absorb in the region 3450–3250 cm^{-1} in solids or liquids and they are broad and of medium intensity. Solid and liquid phases, a band of medium intensity is observed at 3500–3300 cm^{-1} for secondary aromatic amines. In general the vibrational bands due to the N–H stretching are sharper and weaker than those of O–H stretching vibrations by virtue of which they can be easily identified (Gunasekaran *et al.*, 2003; Collins *et al.*, 1998). In the present case the compounds chosen for study is a hetero cyclic aromatic system of pyrimidine and has only one N-H stretching vibration at its side chain substitution. Hence, the band appears at 3460 cm^{-1} in the FTIR spectrum and the band at 3459 cm^{-1} in the FT Raman spectrum of N3BP2MA is assigned to the N-H stretching mode of vibration. The Wavenumbers calculated through B3LYP/6-31G(2d,3p) and B3LYP/6-311++G(2d,3p) methods are in good agreement with the experimental values.

C-H Vibrations

The substituted benzene like molecule gives rise to C–H stretching, C–H in-plane and C–H out-of-plane bending vibration. In the aromatic compounds, the carbon–hydrogen stretching vibrations normally occur at 3250–3000 cm^{-1} (Gunasekaran *et al.*, 2008). Heterocyclic compound C-H vibration absorption bands are usually weak; in many cases it is too weak for detection. The bands due to C–H in-plane bending vibrations interact somewhat with C–C stretching vibrations is observed as a number of bands in the region 1450–1100 cm^{-1} . The C–H out-of-plane bending vibrations occur in the region 900–667 cm^{-1} (Gunasekaran *et al.*, 2008; Puviarasan *et al.*, 2002). In this region the vibrations are not found to be affected due to the nature and position of the substituent (Varsanyi, 1973). In the present work, the bands observed at 3199, 3190, 3181 and 3176 cm^{-1} are assigned to C–H asymmetric vibrations and 3149, 3124, 3094, 3070 cm^{-1} in the N3BP2MA compound have been assigned to C-H symmetric stretching vibration. Apart from the mentioned values other vibrations in the same range are assigned to C-H stretching vibrations respectively. The C-H bending vibrations appear at two distinct regions 1490 - 1300 cm^{-1} and 1100 – 900 cm^{-1} , due to in plane and out of plane bending vibrations respectively (Krishnakumar and John Xavier, 2003; Krishnakumar and Prabavathi, 2008). The band position observed at 1487 cm^{-1} and 1057 cm^{-1} in experimental spectrum of N3BP2MA are assigned to C-H in plane and out of plane bending vibrations. The wave numbers calculated through DFT

techniques are in good agreement with the experimental data (Krishnakumar and John Xavier, 2003).

C-N vibrations

The identification of C-N stretching vibration is a very difficult task, since the mixing of bands is possible in this region. The FT Raman band observed in 1314, 1328 and 1354 cm^{-1} in N3BP2MA have been designated to the C-N stretching mode of vibration. These assignments are made in accordance with the assignment proposed by Bienko, Michalska *et al.* (1999). The C-N stretching band assigned at 1319 cm^{-1} in 2,6-dibromo-4-nitroaniline by Krishna Kumar (2005), Raja *et al.* (1994) have identified the FTIR band at 1342 cm^{-1} due to C-N in theophylline. Gunasekaran *et al.* (2005) have observed the C-N stretching band at 1312 cm^{-1} in benzocaine. The calculated value at 1312, 1328 and 1354 cm^{-1} of N3BP2MA are in excellent agreement with the observed value for the corresponding mode of vibration.

C-C vibrations

The C-C aromatic stretching, vibration gives rise to characteristic bands in both the observed IR and Raman spectra, covering the spectral range from 1600 – 1400 cm^{-1} . The IR bands located at 1595, 1559, 1485 cm^{-1} and 1356 cm^{-1} ; the Raman bands centered at 1593, 1557, 1487 and 1356 cm^{-1} have been assigned to C-C stretching vibrations. Of these bands, 1559 cm^{-1} have appeared characteristically strong in the IR and Raman spectra. The calculated bands at B3LYP level in the same region are in excellent agreement with experimental observations of both in FTIR and FT Raman spectra of N3BP2MA (Gunasekaran *et al.*, 1994; Silverstein *et al.*, 1981). The ring in plane vibrations has given rise to weak bands across the low wavenumber region, that is to say, below 1000 cm^{-1} . The bands at 892 cm^{-1} and at 999 cm^{-1} have been assigned to C-C in plane bending vibrations. As is seen from Table 3 the predicted vibrational bands agree well with the observed ones.

C-S Vibrations

In general the assignment of the band due to C-S stretching vibrations in different compounds is difficult. Both aliphatic and aromatic sulphides have weak to medium band due to C-S stretching in the region 780 - 510 cm^{-1} (Gunasekaran *et al.*, 2003; Roggers, 1994). Double bond conjugation with the C-S band like vinyl or phenyl lowers the C-S stretching frequency and increases the intensity. In view of this the medium intense bands present at 581 and 769 cm^{-1} in the FTIR spectrum of N3BP2MA and the band at 769 cm^{-1} in the FT Raman spectrum of N3BP2MA are assigned to be due to C-S stretching modes of vibrations.

S=O Stretching vibration

In solid phase sulphonamides have a strong, broad absorption band at 1360-1315 cm^{-1} due to the asymmetric stretching vibration of S=O group, whereas the symmetric stretching vibration of this group shows the occurrence at 1280 - 1240 cm^{-1} (Seshadri *et al.*, 2009; Jong Rack Sohn *et al.*, 2001).

Similarly, in the case of dilute solutions in nonpolar solvents, all organic sulphonamides have two strong bands at 1360 – 1290 cm⁻¹ and 1270-1220 cm⁻¹ due to asymmetric and symmetric stretching vibrations respectively. In the present case, the FTIR spectrum of N3BP2MA, shows the presence of the bands due to symmetric and asymmetric stretching of the S=O group at 1229 cm⁻¹ and at 1297 cm⁻¹ respectively.

Other molecular properties

NLO properties

Many organic molecules that contain conjugated π electrons are characterized hyperpolarizabilities have been analyzed by means of vibrational spectroscopy (Thomson and Torkingto, 1945; Glendening *et al.*, 2001). Both the B3LYP/6-31G(2d,3p) and B3LYP/6-311++G(2d,3p) method has been used for the prediction of first order hyperpolarizability (β) of the title compound. The tensor components of the static first order hyperpolarizability (β) were analytically calculated by using the same method as mentioned above. From the computed tensorial components, β is calculated for the title compound by taking into account the Kleimman symmetry relations and the square norm of the Cartesian expression for the β tensor (Reed *et al.*, 1988).

The first order hyperpolarizability (β) of this novel molecular system and the related properties (α_0 and $\Delta\alpha$) of N3BP2MA were calculated, based on the finite field approach. The complete equations for calculating the magnitude of the total static dipole moment μ , the mean polarizability α_0 , the anisotropy of the polarizability $\Delta\alpha$, and the mean first order hyperpolarizability β , using the x, y, z components are defined as follow:

$$\mu = (\mu_x^2 + \mu_y^2 + \mu_z^2)^{1/2}$$

$$\beta = (\beta_x^2 + \beta_y^2 + \beta_z^2)^{1/2}$$

$$\alpha = \frac{\alpha_{xx} + \alpha_{yy} + \alpha_{zz}}{3}$$

$$\Delta\alpha = 2^{-1/2} ((\alpha_{xx} - \alpha_{yy})^2 + (\alpha_{yy} - \alpha_{zz})^2 + (\alpha_{zz} - \alpha_{xx})^2 + 6 \alpha_{xx}^2)^{1/2}$$

Where

$$\beta = \beta_{xxx} + \beta_{xyy} + \beta_{xzz}$$

$$\beta = \beta_{yyy} + \beta_{xxy} + \beta_{yzz}$$

$$\beta = \beta_{zzz} + \beta_{xxz} + \beta_{yyz}$$

The components of polarizability and the first order hyperpolarizability of the title compound can be seen in Table 4. The calculated value of first hyperpolarizability shows that N3BP2MA might have the NLO properties. The nonlinear optical activity provides useful information for frequency shifting, optical modulation, optical switching and optical logic for the developing technologies in areas such as communication, signal processing and optical interconnections.

NBO/NLMO analysis

NBO (Natural Bond Orbital) analysis provides an efficient method for studying intra and inter molecular bonding and interaction among bonds, and also provides a convenient basis for investigation, charge transfer or conjugative interactions in the molecular system (Thomson and Torkingto, 1945). By the use of the second-order bond–antibond (donor–acceptor) NBO energetic analysis, insight in the most important delocalization schemes was obtained. The change in electron density (ED) in the (σ^* , π^*) antibonding orbitals and E(2) energies have been calculated by natural bond orbital (NBO) analysis (Thomson and Torkingto, 1945) using DFT methods to give clear evidence of stabilization originating from various molecular interactions. NBO analysis has been performed on N3BP2MA in order to elucidate intramolecular hydrogen bonding, intramolecular charge transfer (ICT) interactions and delocalization of π -electrons. The hyperconjugative interaction energy was deduced from the second-order perturbation approach (Glendening *et al.*, 2001).

$$E(2) = - \frac{(\sigma|F|\sigma)^2}{\epsilon_{\sigma'} - \epsilon_{\sigma}} n_{\sigma} = \frac{F_{ij}^2}{\Delta E} - n_{\sigma}$$

Where $(\sigma|F|\sigma)^2$ or F_{ij}^2 is the Fock matrix element between the i and j NBOs, ϵ_{σ} and ϵ_{σ^*} are the energies of σ and σ^* NBOs, and n_{σ} is the population of the donor σ orbital.

In Table 5, the perturbation energies of significant donor–acceptor interactions are presented. The larger the E(2) value, the intensive is the interaction between electron donors and electron acceptors. In N3BP2MA, the interactions between antibonding of C9-C14 and the corresponding antibonding of C12–C13 have the high E (2) value around 257.71 kcal/Mol. The other significant interactions, giving stronger stabilization energy value of 237.22 kcal/Mol to the structure is the interactions between antibonding of C18–C23 between the antibonding of C19-C20. Table 5 gives the occupancy of electrons and p-character (Reed *et al.*, 1988) in significant NBO natural atomic hybrid orbital. In C–H bonds, the hydrogen atoms have almost 0% of p-character. The 100% p-character is observed in the first lone pair of N4, N6 and in the third lone pair of O16.

The natural localized molecular orbital (NLMO) analysis has been carried out since they show how bonding in a molecule is composed from orbits localized on different atoms. The derivation of NLMOs from NBOs gives direct insight into the nature of the localized molecular orbital's “delocalization tails” (Reed *et al.*, 1988; Xavier *et al.*, 2012). Table 7 shows significant NLMO's occupancy, percentage from parent NBO and atomic hybrid contributions of N3BP2MA calculated at B3LYP level using 6-31G (2d,3p) basis set. The NLMO of C9-C14 is the most delocalized NLMO occupancy of 79.39% contribution from the localized C9-C14 parent NBO, and the delocalization tail (\approx 19%) consists of the hybrids of C7, C8, C10, C11, C12 and C13.

Table 4. The calculated μ , α and β components of N3BP2MA

Parameters	B3LYP/6-31G(2d,3p)	B3LYP/ 6-311++G(2d,3p)	Parameters	B3LYP/6-31G(2d,3p)	B3LYP/ 6-311++G(2d,3p)
μ_x	0.9074	0.8156	β_{xxx}	466.939	529.632
μ_y	0.4724	0.4167	β_{xxy}	162.884	-98.574
μ_z	-3.9794	-4.2380	β_{xyy}	-70.264	84.201
μ	4.1088	4.7377	β_{yyy}	-51.961	-28.989
α_{xx}	352.206	311.741	β_{xxz}	-48.738	-53.454
α_{xy}	-1.553	-4.117	β_{xyz}	2.094	5.559
α_{yy}	274.150	204.792	β_{yyz}	-8.497	24.715
α_{xz}	6.214	6.750	β_{xzz}	2.867	12.111
α_{yz}	12.455	13.043	β_{yzz}	-0.176	3.607
α_{zz}	73.712	88.437	β_{zzz}	-2.073	2.523
α_{tot}	233.356	201.646	$\beta_{tot}(esu)$	1.43×10^{-30}	1.61×10^{-30}
$\Delta\alpha$	658.932	811.132			

Table 5. Second order perturbation theory, analysis of Fock matrix in NBO basis of N3BP2MA

Donor(i)	Acceptor(J)	E ² kcal/mol	E(j)-E(i) a.u	F(i,j)a.u
LP(1) N4	π^*C1-O3	52.90	0.32	0.117
LP(1)N6	π^*C7-C8	32.67	0.30	0.089
LP(1)N6	$\pi^*C9-C14$	27.55	0.31	0.086
LP(3)O16	$\sigma^*N6-S15$	23.75	0.37	0.086
π^*C7-C8	$\pi^*C9-C14$	165.85	0.01	0.061
$\pi^*C9-C14$	$\pi^*C10-C11$	207.42	0.02	0.081
$\pi^*C9-C14$	$\pi^*C12-C13$	257.71	0.01	0.081
$\pi^*C18-C23$	$\pi^*C19-C20$	237.22	0.01	0.077
$\pi^*C18-C23$	$\pi^*C21-C22$	211.89	0.01	0.085

^a E(2) means energy of hyper conjugative interaction (stabilization energy).

^b Energy difference between donor and acceptor i and j NBO orbitals.

^c F(i, j) is the fork matrix element between i and j NBO orbitals.

Table 6. Occupancy, percentage of p character of significant natural atomic hybrid of the natural bond orbital of N3BP2MA calculated at B3LYP/6-311++ G(2d,3p)

Bond	ED(e)	Hybrid	Atom	p.%
BD(2) C7-C8	1.8771	0.6760(sp1.00)C+0.7369(sp1.00)C	C7	99.92
BD(2)C9-C14	1.60940	0.7105(sp1.00)C+0.7037(sp1.00)C	C9	99.97
BD(2)C10-C11	1.71593	0.7045(sp1.00)C+0.7097(sp1.00)C	C10	99.95
BD(2)C18-C23	1.68005	0.7601(sp1.00)C+0.6498(sp1.00)C	C18	99.98
BD(2)C19-C20	1.65157	0.6983(sp1.00)C+0.7158(sp1.00)C	C19	99.96
BD(2)C21-C22	1.63734	0.7008(sp1.00)C+0.7134(sp1.00)C	C21	99.96
LP(1) N4	1.69767	p1.00	N4	99.72
LP(1)N6	1.66327	p1.00	N6	99.94
LP(3) O16	1.76772	p1.00	O16	99.68
BD(2) C7-C8	0.31919	0.7369(sp1.00)C-0.6760(sp1.00)C	C7	99.92
BD(2)C9-C14	0.47635	0.7037(sp1.00) C-0.7105(sp1.00)C	C9	99.97
BD(2)C10-C11	0.30065	0.7097(sp1.00)-0.7045(sp1.00)C	C10	99.95
BD(2)C18-C23	0.38319	0.6498(sp1.00)C-0.7601(sp1.00)C	C18	99.98
BD(2)C19-C20	0.30728	0.7158(sp1.00)-0.6983(sp1.00)C	C19	99.96
BD(2)C21-C22	0.31023	0.7134(sp1.00)C-0.7008(sp1.00)	C21	99.96

Table 7. Significant NLMO's occupancies, percentage from parent NBO and atomic hybrid contributions of N3BP2MA calculated using B3LYP/6-311++G (2d,3p) basis set

Bond	Occupancy	% from Parent NBO	Hybrid contributions	
			Atom	%
BD(2)C9-C14	2.00000	79.39	C7	2.540
			C8	2.068
			C10	6.279
			C11	2.068
			C12	3.214
			C13	3.563
BD(2)C19-C20	2.00000	81.9060	C18	3.389
			C21	8.124
			C22	2.083
			C23	4.387
			C18	4.446
			C19	4.171
BD(2)C21-C22	2.00000	80.1715	C20	4.194
			C23	6.549

Molecular electrostatic potential

Molecular electrostatic potential and electrostatic potential is useful quantities to illustrate the charge distributions of molecules and used to visualize variably charged regions of a molecule. Therefore, the charge distributions can give information about how the molecules interact with another molecule. The molecular electrostatic potential is widely used as a reactivity map displaying most probable regions for the electrophilic attack of charged point-like reagents on organic molecules (Politzer and Truhlar, 1981). The molecular electrostatic potential $V(r)$ that is created in the space around a molecule by its nuclei and electrons is well established as a guide to molecular reactive behavior. It is defined by:

$$V(r) = \sum_A \frac{Z_A}{(R_A - r)} - \int \frac{\rho(r')}{(r' - r)} dr'$$

in which Z_A is the charge of nucleus A, located at R_A , $\rho(r')$ is the electron density function of the molecule and r' is the dummy integration variable (Politzer *et al.*, 1985). At any given point $r(x, y, z)$ in the vicinity of a molecule, the molecular electrostatic potential (MEP), $V(r)$ is defined in terms of the interaction energy between the electric charge generated from the molecule's electrons and nuclei and a positive test charge (a proton) located at r (Politzer and Murray, 2002).

charges contribution or positive charges contribution. Accordingly, it is possible to identify regions more susceptible to an approximation of electrophilic molecules or nucleophilic molecules, so the molecular electrostatic potential map is commonly used as reactivity map. To predict regions more susceptible to approximation of either electrophiles or nucleophiles, MESP was calculated at the B3LYP/6-31G (2d,3p) is shown in Fig. 5. The importance of total electron density surface mapped with the electrostatic potential lies in the fact that it simultaneously displays molecular size, shape, as well as positive or negative electrostatic potential regions in terms of color grading and is very useful in research of molecular structure with its physiochemical property relationship (Okulik and Jubert, 2005).

The different values of the electrostatic potential are represented by different colors. The range values for the color scale of the mapped MESP should be symmetrical to allow easy identification of negative (red) and the positive (blue) potential regions. The use of a symmetrical potential scale values eases the recognition of positive, zero or negative regions. In GaussView visualizing program (Rauhut and Pulay, 1995) the following spectral color scheme is used. So potential increases in the order: red < orange < yellow < green < cyan < blue. Therefore red indicates negative regions, blue indicates positive regions, while green appears over zero electrostatic potential regions.

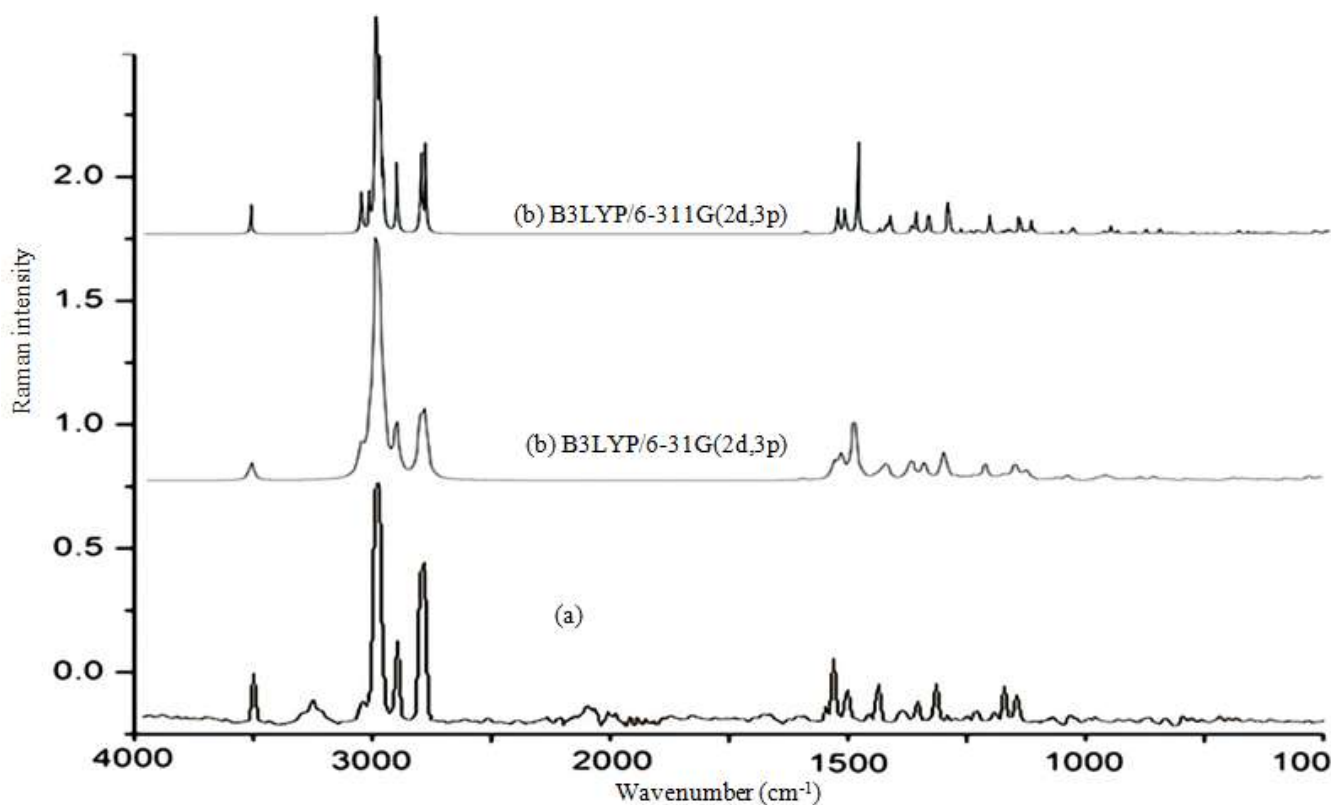


Fig. 4. Comparative (a) Experimental and (b) Theoretical Raman spectra of N3BP2MA

In the graphic of total electron density surface mapped with the electrostatic potential, the sign of the electrostatic potential in a surface region is determined by the predominance of negative

It is accepted that the negative (red) and the positive (blue) potential regions in the mapped MESP represent regions

susceptible to approach electrophilic molecules or nucleophilic molecules, respectively.

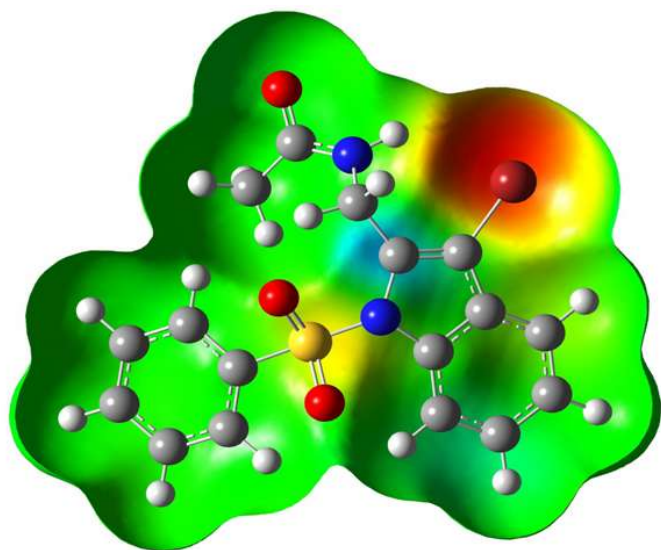


Fig.5. Molecular electrostatic potential of N3BP2MA

It can be seen that the most possible sites for electrophilic attack is H15. Negative regions of the studied molecule are found around the C5, C6 and C7 atoms indicating a possible site for nucleophilic attack. According to these calculated results, the MEP map shows that the negative potential sites are on electronegative atoms as well as the positive potential sites are around the hydrogen atoms. The contour map provides a simple way to predict how different geometries could interact and is shown in Fig. 6.

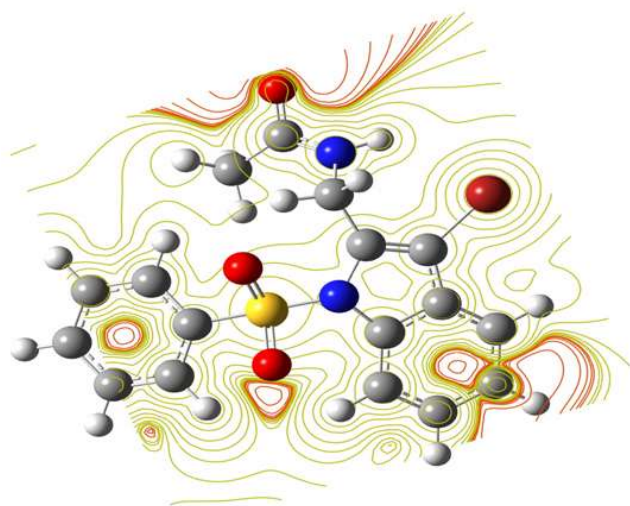


Fig. 6. The contour map of electrostatic potential of the total density of N3BP2MA

Mulliken Charge distribution

The Mulliken populations show one of the simplest pictures of charge distribution. The Mulliken charges provide net atomic populations in the molecule while electrostatic potentials yield the electric field out of the molecule produced by the internal charge distribution. Thus, in the reactivity studies, Mulliken

populations and MESP are complementary tools, and correlation between the schemes is expected (Mulliken, 1955). However, Mulliken population analysis requires very careful because problems as large changes of the calculated atomic charges with small changes in the bases used and the overestimation of the covalent character of a bond are common. So, in general, the absolute magnitude of the atomic charges has little physical meaning, on the other hand, their relative values can offer valuable information. The Mulliken charge distribution of the molecule was calculated at B3LYP level with 6-31G (d,p) and 6-311++G(d,p) basis sets. Mulliken charge distribution graphically and structurally is shown in Figs. 7 & 8. The total atomic charges of N3BP2MA using B3LYP/6-31G(2d,3p) and B3LYP/6-311++G(2d,3p) methods were listed in Table 8.

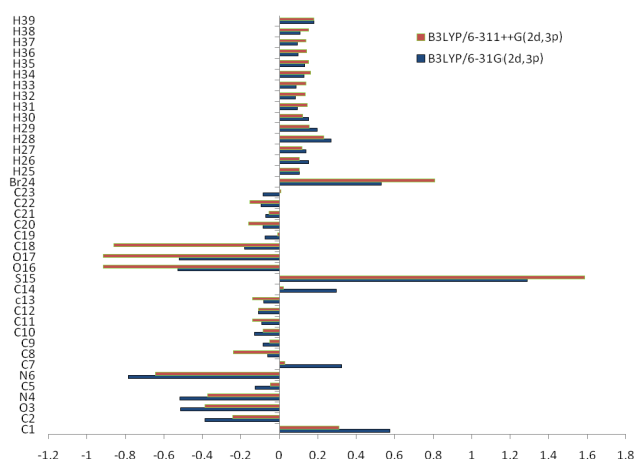


Fig. 7. Histogram of calculated Mulliken atomic charges of N3BP2MA

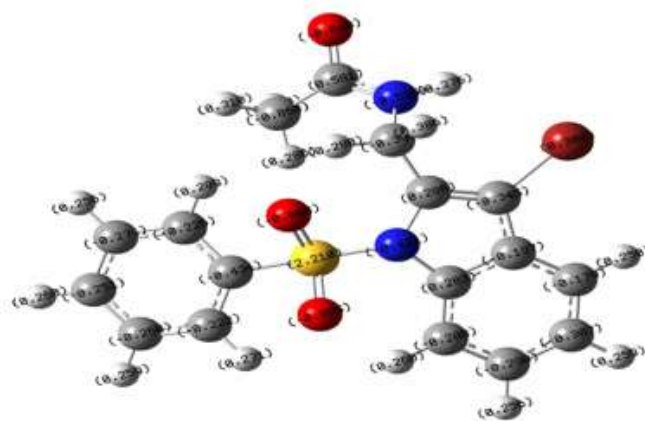


Fig. 8. Structural charge distribution of N3BP2MA

For Mulliken charge distribution, the GaussView adopts the follow colors scheme: bright red for more negative charge and bright green for a more positive charge. The red hues illustrate negative charges while green hues expose positive charges. The charge distribution of the compound shows that carbon atom (C18) attached with sulphur and carbon atoms has negative charges. All the hydrogen atoms have positive Mulliken charges. The atom C1 has the highest Mulliken charge (0.574488) when compared to other atoms. The Sulphur

element present in the compound S15 has a maximum positive value of 1.585617. The nitrogen (N6) atoms are much more negative charge than the other atoms. The smallest Mulliken charge value (-0.373985) was obtained for N4 atom. The Mulliken charge distribution and the MESP information are concordant.

Global and local reactivity descriptors

The Highest Occupied Molecular Orbitals (HOMOs) and Lowest-Lying Unoccupied Molecular Orbitals (LUMOs) are named as Frontier molecular orbitals (FMOs). The energy gap between the HOMOs and LUMOs is the critical parameters in determining molecular electrical transport properties helps in the measure of electron conductivity. To understand the bonding feature of the title molecule, the plot of the Frontier orbitals, the highest occupied molecular orbital HOMO and lowest unoccupied molecular orbital LUMO as shown in Fig. 9. The HOMO shows that the charge density localized mainly on carbonyl and amine group where as LUMO is localized on ring system. Gauss-Sum 2.2 Program (Boyle *et al.*, 2008) has been used to calculate group contributions to the molecular orbitals and prepare the density of the state (DOS) as shown in Fig. 10. The DOS spectra were created by convoluting the molecular orbital information with GAUSSIAN curves of the unit height.

By using HOMO and LUMO energy values for a molecule, the global chemical reactivity descriptors of molecules such as hardness, chemical potential, softness, electronegativity and electrophilicity index as well as local reactivity have been defined (Parr *et al.*, 1999; Chattaraj *et al.*, 2003; Parr *et al.*, 1978; Parr *et al.*, 1983; Parr *et al.*, 1991). Pauling introduced the concept of electronegativity as the power of an atom in a molecule to attract electrons to it. Hardness (η), chemical potential (μ) and electronegativity (χ) and softness are defined follows.

$$\eta = \frac{1}{2} \left(\frac{\partial^2 E}{\partial N^2} \right) V(r) = \frac{1}{2} \left(\frac{\partial \mu}{\partial N} \right) V(r)$$

$$\mu = \left(\frac{\partial E}{\partial N} \right) V(r)$$

$$\chi = -\mu = - \left(\frac{\partial E}{\partial N} \right) V(r)$$

Where E and V (r) are electronic energy and external potential of an N-electron system respectively. Softness is a property of a molecule that measures the extent of chemical reactivity. It is the reciprocal of hardness.

Table 8. Mullikan atomic charges table of N3BP2MA

Atom	B3LYP/ 6-31G(2d,3p)	B3LYP/6-311++G(2d,3p)	Atom	B3LYP/6-31G(2d,3p)	B3LYP/6-311++G(2d,3p)
C	0.574488	0.308706	C	-0.072493	-0.055714
C	-0.388436	-0.242417	C	-0.097093	-0.152704
O	-0.514719	-0.385570	C	-0.085224	0.006153
N	-0.517390	-0.373985	Br	-0.128683	0.806072
C	-0.125265	0.004706	H	0.102381	0.102874
N	-0.784547	-0.644055	H	0.152438	0.104554
C	0.323756	0.027718	H	0.137020	0.117897
C	-0.062145	-0.240330	H	0.267451	0.231828
C	0.084416	-0.050191	H	0.196671	0.155820
C	-0.130315	-0.086081	H	0.152379	0.120388
C	-0.090837	-0.141734	H	0.094688	0.145239
C	-0.109729	-0.109688	H	0.082121	0.135119
C	-0.081236	-0.138568	H	0.087375	0.136326
C	0.295784	0.020034	H	0.128130	0.161680
S	1.288529	1.585617	H	0.131463	0.151885
O	-0.528675	-0.914853	H	0.097775	0.142589
O	-0.520057	-0.916191	H	0.093025	0.138166
C	-0.180122	-0.861344	H	0.108150	0.151509
C	-0.074685	-0.010377	H	0.180491	0.179817
C	-0.086879	-0.161459			

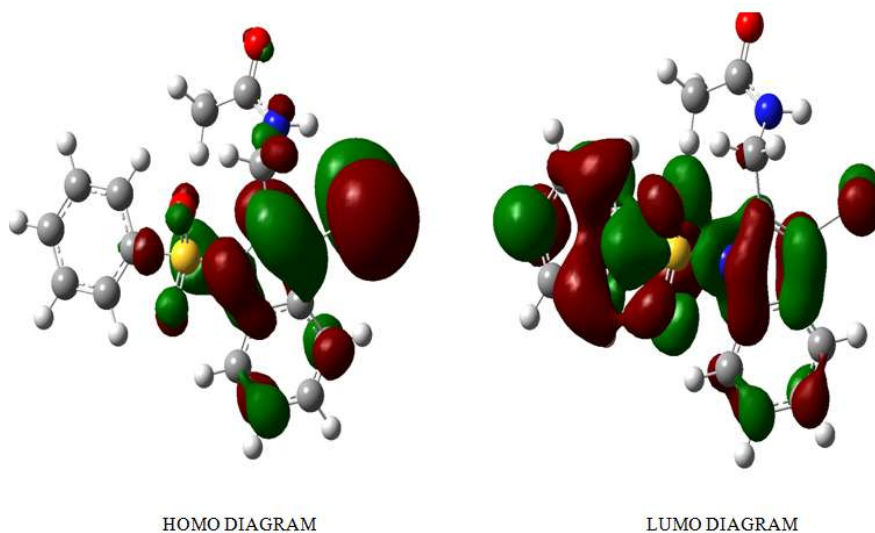


Fig. 9. Frontier molecular orbital N3BP2MA

$$S = \frac{1}{\eta}$$

Using Koopman's theorem for closed-shell molecules, η , μ and χ can be defined as

$$\eta = \frac{I-A}{2} \quad \mu = \frac{-(I+A)}{2} \quad \chi = \frac{I+A}{2}$$

Where A and I are the ionization potential and electron affinity of the molecules respectively. The ionization energy and electron affinity can be expressed through HOMO and LUMO orbital energies as $I = -E_{\text{HOMO}}$ and $A = -E_{\text{LUMO}}$. Electron affinity refers to the capability of a ligand to accept precisely one electron from a donor. The ionization potential calculated by B3LYP/6-31G(2d,3p) and B3LYP/6-311++G(2d,3p) methods for N3BP2MA is 7.8119 eV and 4.6017 eV respectively. Considering the chemical hardness, large HOMO–LUMO gap means a hard molecule and small HOMO–LUMO gap means a soft molecule.

One can also relate the stability of the molecule to hardness, which means that the molecule with least HOMO–LUMO gap means it, is more reactive. Recently Parr *et al.* (1999) has defined a new descriptor to quantify the global electrophilic power of the molecule as an electrophilicity index (ω), which defines a quantitative classification of the global electrophilic nature of a molecule Parr *et al.* (1999) have proposed electrophilicity index (ω) as a measure of energy, lowering due to maximal electron flow between donor and acceptor. They defined electrophilicity index (ω) as follows:

$$\omega = \frac{\mu^2}{2}$$

Using the above equations, the chemical potential, hardness and electrophilicity index have been calculated for N3BP2MA and their values are shown in Table 9. The usefulness of this new reactivity quantity has been recently demonstrated in understanding the toxicity of various pollutants in terms of their reactivity and site selectivity (Parthasarathi *et al.*, 2004; Parthasarathi *et al.*, 2004; Parthasarathi *et al.*, 2003; Irikura, 2002). The calculated value of electrophilicity index describes the biological activity of N3BP2MA.

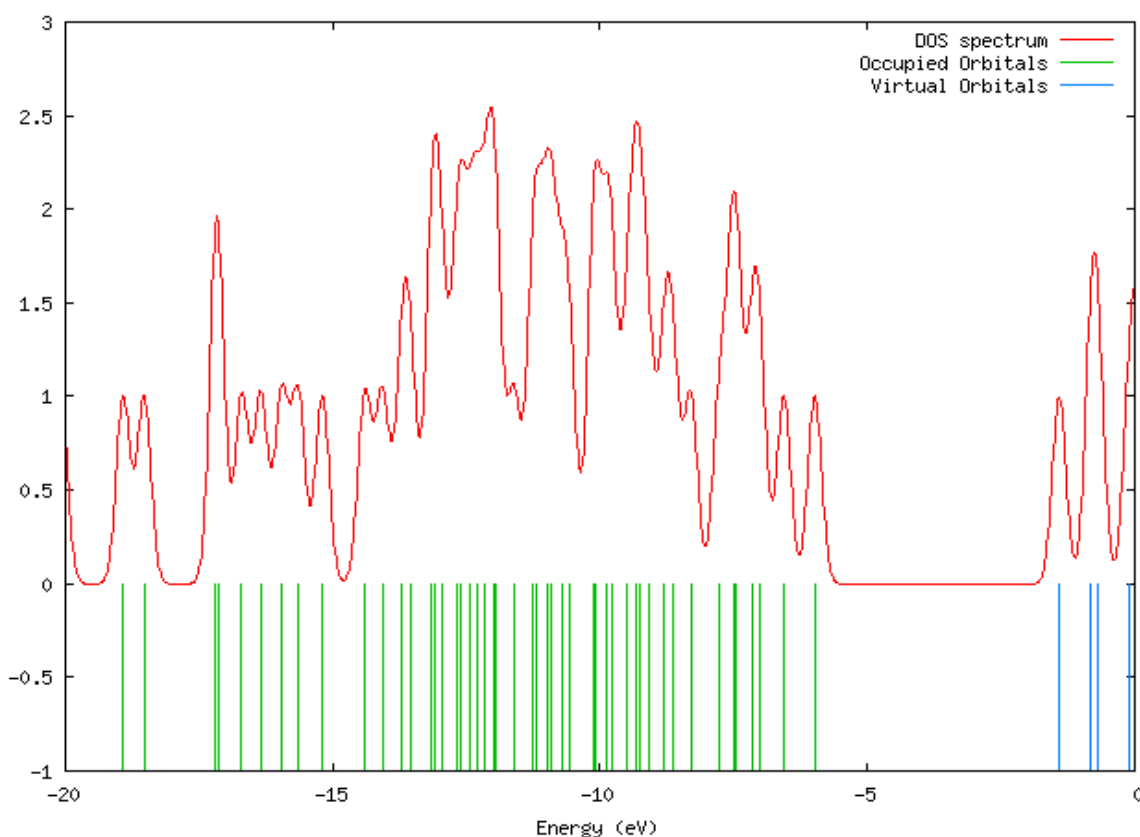


Fig. 10. DOS spectrum of N3BP2MA

Table 9. Molecular properties of N3BP2MA

Molecular properties	B3LYP		Molecular properties	B3LYP	
	6-31G(2d,3p)	6-311++G(2d,3p)		6-31G(2d,3p)	6-311++G(2d,3p)
E_{HOMO} (eV)	-8.8922	-5.9628	Chemical hardness(η)	3.9046	2.3008
E_{LUMO} (eV)	-1.0830	-1.3611	Softness(S)	0.2561	0.4346
$E_{\text{HOMO-LUMO}}$ gap(eV)	7.8119	4.6017	Chemical potential(μ)	-4.9876	-3.6619
Ionisation potential(I)eV	8.8922	5.9628	Electronegativity (χ)	4.9876	3.6619
Electron affinity(A)eV	1.0830	1.3611	Electrophilicity index (ω)	12.4380	6.7048

Table 10. Thermo dynamical properties of N3BP2MA

T (K)	S (J/mol.K)		C _p (J/mol.K)		ddH (kJ/mol)	
100	430.41	417.45	154.94	151.58	9.93	9.82
200	568.21	551.11	253.92	248.41	30.37	30.03
298.15	687.99	667.28	352.53	344.88	60.14	59.46
300	690.18	669.41	354.36	346.67	60.79	60.10
400	805.25	781.01	448.10	438.38	101.02	99.88
500	914.02	886.51	527.07	515.63	149.91	148.22
600	1015.96	985.38	590.69	577.87	205.92	203.59
700	1110.99	1077.55	641.76	627.83	267.63	264.61
800	1199.49	1163.39	683.27	668.44	333.95	330.18
900	1282.00	1243.41	717.52	701.95	404.04	399.47
1000	1359.13	1318.22	746.15	729.96	477.27	471.88

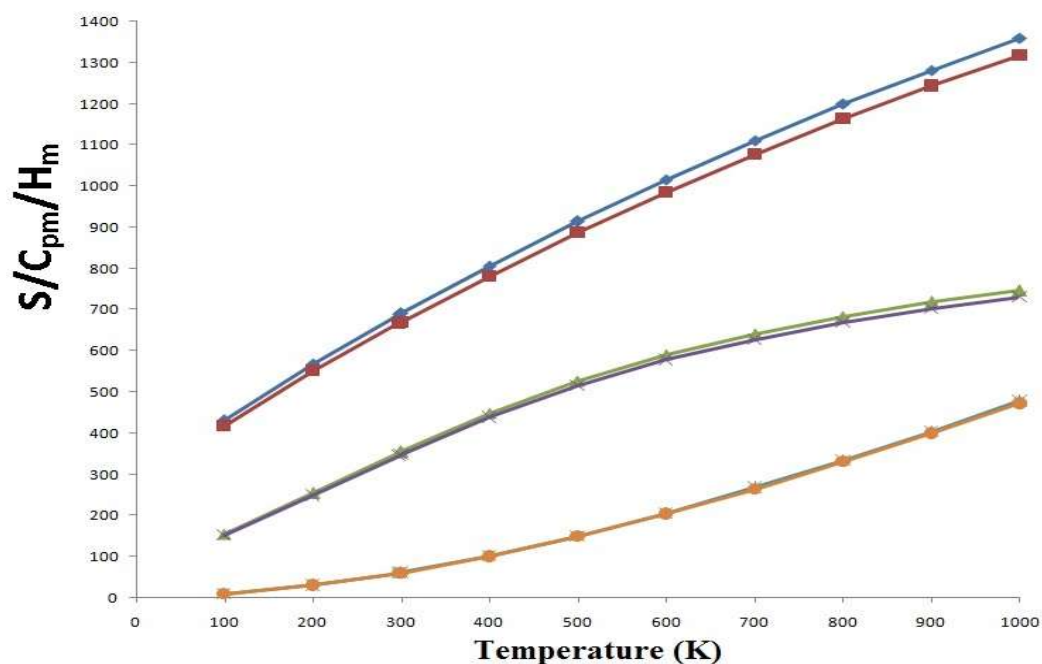


Fig. 11. Thermodynamical properties of N3BP2MA by B3LYP/6-31G(2d,3p) and B3LYP/6-311++G(2d,3p)

Temperature dependence of thermodynamic properties

The statistical thermodynamics, like the standard thermodynamic functions such as heat capacity, entropy and enthalpy were calculated using perl script THERMO.PL (Irikura, 2002) and are listed in Table 10. As observed from the Table 7, the values of C_p , H and S all increase with the increase of temperature from 100 to 1000 K, which is attributed to the enhancement of the molecular vibration as the temperature increases. The correlation equations between heat capacity (C_{pm}°), entropy (S_m°), enthalpy (H_m°) changes and temperatures were fitted by quadratic formulas and the corresponding fitting factors (R^2) for these thermodynamic properties are 0.9999, 0.9998 and 0.9998, respectively. The corresponding fitting equations are as follows and the correlation graphs of those shown in Fig. 11.

$$S_m^{\circ} = 240.03433 + 0.7328 T - 1.79433 \times 10^{-4} T^2 \quad (R^2 = 0.9999)$$

$$C_{pm}^{\circ} = 15.26587 + 0.65639 T - 2.82786 \times 10^{-4} T^2 \quad (R^2 = 0.9998)$$

$$H_m^{\circ} = -7.65942 + 0.08696 T + 1.73344 \times 10^{-4} T^2 \quad (R^2 = 0.9998)$$

All the thermodynamic data provide helpful information to further study of the title compounds. They compute the other

thermodynamic energies according to the relationship of thermodynamic functions and estimate directions of chemical reactions according to the second law of thermodynamics in thermo chemical field.

Notice: all thermodynamic calculations were done in gas phase and they could not be used in solution.

Conclusion

A complete structural, thermodynamic, first-order hyperpolarizability, Mulliken population analysis, vibrational and electronic investigations of N3BP2MA have been carried out with FTIR and FT-Raman spectroscopic technique along with a DFT/B3LYP method with different basis sets. The gas phase structure and conformational properties of N3BP2MA and its conformers were determined by quantum chemical calculations. It is found that molecule has twelve conformers. The equilibrium geometries and harmonic frequencies of N3BP2MA was determined and analyzed at the DFT level utilizing B3LYP/6-31G(2d,3p) and B3LYP/6-311++G(2d,3p) basis set, giving allowance for the lone pairs through diffuse

functions. The difference between observed and calculated wavenumber values of the most of the fundamental modes is very small. Any discrepancy noted between the observed and the calculated vibrational band assignments may be due to the fact that the calculations have been actually done on a single molecule in the gaseous state contrary to the experimental values recorded in the presence of intermolecular interactions. The various intramolecular interactions that are responsible for the stabilization of the molecule was revealed by the natural bond orbital analysis. The lowering of HOMO and LUMO energy gap clearly explicates the charge transfer interactions taking place within the molecule.

REFERENCES

- Abkowicz-Bienko A.J., Z. Latajka, D.C. Bienko, D. Michalska, *Chem. Phys.* (1999), 250: 123.
- Andreani A., M. Granaiola, A. Leoni, A. Locatelli, R. Morigi, M. Rambaldi, G. Giorgi, L. Salvini, V. Garaliene (2001). *Anticancer Drug. Des.* 16, 167–174.
- Becke A.D., *J. Chem. Phys.* 98 (1993) 5648–5652.
- Chattaraj P.K., B. Maiti, U. Sarkar, *J. Phys. Chem. A* 107 (2003) 4973–4975.
- Collins G.E., L.S. Chori, J.H. Chllahan, *J. Am. Chem. Soc.*, 1998:120;1474.
- Fogarasi G., P. Pulay, J.R. Durig (Eds.), *Vibrational Spectra and Structure*, vol. 14, Elsevier, Amsterdam, 1985, p. 125 (Chapter 3).
- Fogarasi G., X. Zhou, P.W. Taylor, P. Pulay, *J. Am. Chem. Soc.* 114 (1992) 8191–8201.
- Frisch A., A.B. Nielson, A.J. Holder, *Gaussview Users Manual*, Gaussian Inc., Pittsburgh, PA, 2000.
- Frisch M.J., G.W. Trucks, H.B. Schlegel, G.E. Scuseria, M.A. Robb, J.R. Cheeseman, J.A. Montgomery Jr., T. Vreven, K.N. Kudin, J.C. Burant, J.M. Millam, S.S. Iyengar, J. Tomasi, V. Barone, B. Mennucci, M. Cossi, G. Scalmani, N. Rega, G.A. Petersson, H. Nakatsuji, M. Hada, M. Ehara, K. Toyota, R. Fukuda, J. Hasegawa, M. Ishida, T. Nakajima, Y. Honda, O. Kitao, H. Nakai, M. Klene, X. Li, J.E. Knox, H.P. Hratchian, J.B. Cross, V. Bakken, C. Adamo, J. Jaramillo, R. Gomperts, R.E. Stratmann, O. Yazyev, A.J. Austin, R. Cammi, C. Pomelli, J.W. Ochterski, P.Y. Ayala, K. Morokuma, G.A. Voth, P. Salvador, J.J. Dannenberg, V.G. Zakrzewski, S. Dapprich, A.D. Daniels, M.C. Strain, O. Farkas, D.K. Malick, A.D. Rabuck, K. Raghavachari, J.B. Foresman, J.V. Ortiz, Q. Cui, A.G. Baboul, S. Clifford, J. Cioslowski, B.B. Stefanov, G. Liu, A. Liashenko, P. Piskorz, I. Komaromi, R.L. Martin, D.J. Fox, T. Keith, M.A. Al-Laham, C.Y. Peng, A. Nanayakkara, M. Challacombe, P.M.W. Gill, B. Johnson, W. Chen, M.W. Wong, C. Gonzalez, J.A. Pople *Gaussian 03W Program*, Gaussian Inc., Wallingford, CT, 2004.
- Glending E.D., J.K. Badenhoop, A.E. Reed, J.E. Carpenter, J.A. Bohmann, C.M. Morales, F. Weinhold, NBO 5.0, *Theoretical Chemistry Institute, University of Wisconsin, Madison*, 2001.
- Gunasekaran S., P. Kumaresan, K. Manoharan, S. Mohan, *Asian J. Chem.* (1994), 6, 821–826
- Gunasekaran S., R.K. Natarajan, K. Santhosam, *Asian J. Chem.*, 2003:15;1347
- Gunasekaran S., R.K. Natarajan, R. Rathika, D. Syamala, *Ind. J. Phys.* 79(2005) 509–515.
- Gunasekaran S., S. Seshadri, S. Muthu, S. Kumaresan, R. Arunbalaji, *Spectrochim. Acta A* 70 (2008) 550–556.
- Gunasekaran S., U. Ponnambalam, S. Muthu, L. Mariappan, *Asian J. Phys.*, (2003), 16, 1, 51.
- Irikura K.K., THERMO.PEEL Script, National Institute of Standards and Technology, 2002.
- Jong Rack Sohn, Won Cheon Park, *Bull. Korean Chem. Soc.*, (2001), 22, 12, 1297–1298.
- Krishnakumar V., R. John Xavier, *Indian J. Pure Appl. Phys.* 41 (2003) 597–602.
- Krishnakumar V., V. Balachandran, *Spectrochim. Acta, A* 61(2005)1811–1819.
- Krishnakumar V., V.N. Prabavathi, *Spectrochim. Acta, Part A* 71 (2008) 449–457.
- Lee C., W. Yang, R.G. Parr, *Phys. Rev. B* 37 (1988) 785–789.
- MOLVIB (V.7.0): Calculation of Harmonic Force Fields and Vibrational Modes of Molecules, QCPE Program No. 807, 2002.
- MOLVIB (V.7.0): Calculation of Harmonic Force Fields and Vibrational Modes of Molecules, QCPE Program No. 807, 2002.
- Mulliken R.S., *J. Chem. Phys.* 23 (1955) 1833–1841.
- O'Boyle N.M., A.L. Tenderholt, K.M. Langer, *J. Comput. Chem.* 29 (2008) 839–845.
- Okulik N., A.H. Jubert, *Internet Electron, J. Mol. Des.* 4 (2005) 17–30.
- Parr R.G., L. Szentpaly, S. Liu, *J. Am. Chem. Soc.* 121 (1999) 1922–1924.
- Parr R.G., P.K. Chattaraj, *J. Am. Chem. Soc.* 113 (1991) 1854–1855.
- Parr R.G., R.A. Donnelly, M. Levy, W.E. Palke, *J. Chem. Phys.* 68 (1978) 3801–3807.
- Parr R.G., R.G. Pearson, *J. Am. Chem. Soc.* 105 (1983) 7512–7516.
- Parthasarathi R., J. Padmanabhan, M. Elango, V. Subramanian, P. Chattaraj, *Chem. Phys. Lett.* 394 (2004) 225–230.
- Parthasarathi R., J. Padmanabhan, V. Subramanian, B. Maiti, P. Chattaraj, *Curr. Sci.* 86 (2004) 535–542.
- Parthasarathi R., J. Padmanabhan, V. Subramanian, U. Sarkar, B. Maiti, P. Chattaraj, *Internet Electron. J. Mol. Des.* 2 (2003) 798–813.
- Politzer P., D.G. Truhlar (Eds.), *Chemical Application of Atomic and Molecular Electrostatic Potentials*, Plenum, New York, 1981.
- Politzer P., J.S. Murray, *Theor. Chem. Acc.* 108 (2002) 134–142.
- Politzer P., P.R. Laurence, K. Jayasuriya, *Molecular electrostatic potentials: an effective tool for the elucidation of biochemical phenomena*, in: J. McKinney (Ed.), *Structure Activity Correlation in Mechanism Studies and Predictive Toxicology*, *Environ. Health Perspect*, vol. 61, 1985, pp. 191–202.
- Pomarnacka E., I. Kozlarska-Kedra, (2003). *Il Farmaco*, 58, 423–429.
- Pulay P., G. Fogarasi, G. Pongor, J.E. Boggs, A. Vargha, *J. Am. Chem. Soc.* 105 (1983) 7037–7047.
- Puviarasan N., V. Arjunan, S. Mohan, *Turk. J. Chem.* 26 (2002) 323–334.

- Ramathilagam C., P. R. Umarani, V. Saravanan, A. K. Mohanakrishnan, B. Gunasekaran V. Manivannan, Acta Cryst.(2014). E70, o295–o296
- Rauhut G., P. Pulay, J. Phys. Chem. 99 (1995) 3093–3100.
- Reed A.E., L.A. Curtiss, F. Weinhold, Chem. Rev. 88 (1988) 899–926.
- Roggers P.G., A guide to the complete interpretation of Infrared spectra of organic structures, Wiley, Canada, 1994.
- Seshadri S., S. Gunasekaran, S. Muthu, J. Raman Spec, (2009),40,639-644.
- Silverstein M., G. Clayton Basseler, C. Morill, Spectrometric identification of Organic compounds, Wiley, New York, 1981.
- Sing N.P., R.A. Yadav, Ind. J. Phys. 2001; B 75 (4): 347.
- Singh U.P., B. Sarma, P. K. Mishra, A.B. Ray, (2000). Fol. Microbiol. 45, 173–176
- Srivastava A., S.N. Pandeya, (2011). J. Curr. Pharm. Res. 1, 1–17.
- Sundius T., J. Mol. Struct. 218 (1990) 321–326.
- Sundius T., J. Mol. Struct. 218 (1990) 321–326.
- Sundius T., Vib. Spectrosc. 29 (2002) 89–95.
- Sundius T., Vib. Spectrosc. 29 (2002) 89–95.
- Thomson H.W., P. Torkington, J. Chem. Soc. 171 (1945) 640–646.
- Umadevi M., V. Saravanan, R. Yamuna, A.K. Mohanakrishnan, G. Chakkaravarthi, (2013). Acta Cryst. E69, o1784.
- Varsanyi G., Assignments for Vibrational spectra of Seven Hundred Benzene derivatives, ½ Academic Kiaclo, Budapest, 1973.
- Xavier J, Raja S, William S, Gunasekaran S, *Orient.J Chem*, 10 (1994) 3-10.
- Xavier R.J., E. Gobinath, Spectrochim. Acta A 91 (2012) 248–255.
